Nanoscale

Accepted Manuscript

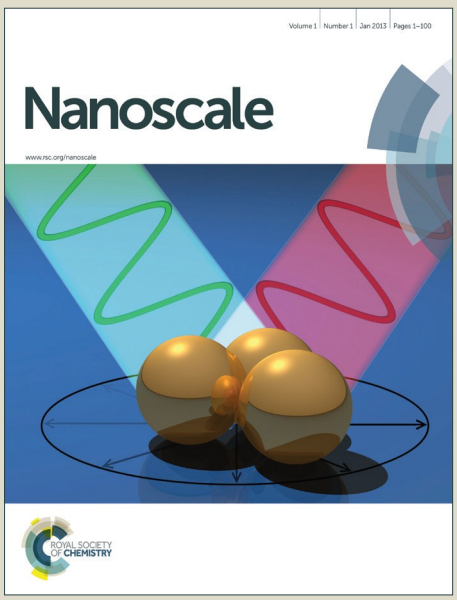

ROYAL SOCIETY OF CHEMISTRY

www.rsc.org/nanoscale

Journal Name

ARTICLE

Direct Carbonization of Cobalt-doped NH_2-MIL-53(Fe) for Electrocatalysis of Oxygen Evolution Reaction

Received 00th January 20xx,
Accepted 00th January 20xx

DOI: 10.1039/x0xx00000x

www.rsc.org/

*Yujie Han[a,b], Junfeng Zhai[a], Lingling Zhang[a,b], and Shaojun Dong[a,b]**

In this work, we synthesized high-performance electrocatalysts for oxygen evolution reaction (OER) by one-step carbonization of cobalt(Co)-doped NH_2-MIL-53(Fe) with different molar ratios between Fe and Co. The results showed that the as-prepared composite with a molar ratio between Fe and Co = 1:3 and the calcination temperature of 550 °C displayed the best OER activity, denoted as MOF(Fe_1-Co_3)$_{550N}$. The MOF(Fe_1-Co_3)$_{550N}$ exists microporous structure with a high Brunauer-Emmett-Teller (BET) surface area of 235.37 $m^2 \cdot g^{-1}$. It shows excellent OER catalytic behavior in 0.1 M KOH solution. The overpotential at 10 $mA \cdot cm^{-2}$ is 0.39 V and the Tafel slope is 54.86 $mV \cdot dec^{-1}$, which is comparable to that of the as-synthesized RuO_2. The satisfied results are attributed to the presence of pyridine N, Co_3O_4, the enlarged surface area and the micropores structures after calcination.

Introduction

The growing demand for energy and the increasing concern about environment pollution from the combustion of coal, oil, and natural gas has boosted the research of diverse kinds of sustainable and environmental friendly energy conversion and storage modes. The splitting of water to produce O_2 (oxygen evolution reaction, OER) and H_2 (hydrogen evolution reaction, HER) either electrochemically or photoelectrochemically is hopeful to meet the energy requirement on a global scale and slow down the current environment pollution resulted from the mass consumption of fossil sources. However, the electrochemical splitting of water is kinetically sluggish in both acidic and alkaline media, and generally needs a large overpotential[1]. Therefore, it is important to employ highly active catalysts to decrease the overpotential and thus achieve efficient water splitting. Hence, a high-performance electrocatalyst is needed to promote the reaction kinetics and decrease the large overpotential and then high energy conversion efficiency can be obtained. IrO_2 and RuO_2 are considered as the most efficient and stable catalyst both in acidic and alkaline solutions[2]. However, Ir and Ru are rare elements with high expense which restricts their wide applications. Recent researches have shown that cobalt (Co) is a promising catalyst for OER with acceptable overpotential both in neutral and alkaline solutions among other kinds of non-noble metal, such as $LiCo_{0.8}Fe_{0.2}O_2$[3] and $LiCo_{0.33}Ni_{0.33}Fe_{0.33}O_2$[4], 3d (M(Ni,Co,Fe,Mn) hydr(oxy)oxide catalysts[5], Co-Pi composites materials[6], chalcogenides[7], Co doped perovskites [8], and molecular catalysts[9]. More interestingly, many studies indicated that the combination of Co with other functional materials could show better OER performance than Co compounds only[10].Because the activities of transition-metal based catalysts for OER were proposed to relate to the number of 3d-electrons in the transition metal ions, the enthalpy of formation of the transition metal hydroxides, and the surface oxygen binding energy[11]. Moreover, the e_g orbital of surface transition metal ions participate in bonding with surface-anion adsorbates, and the occupancy of e_g orbital can greatly influence the binding of oxygen-related intermediate species on surface-anion adsorbates and thus the OER activity[12].

Metal–organic frameworks (MOFs) are a new class of porous crystalline inorganic–organic hybrid materials synthesized by combining metal ions and organic ligands in an appropriate way and have drawn great attention in recent years[13]. Because of the excellent properties of large surface area, tunable pore size, attracting electrical, optical, and catalytic properties, MOFs have shown a variety of potential applications such as heterogeneous catalysis[14], gas storage and separation[15], and drug delivery/release[16]. The metal centers and metal-oxo units in MOFs act as effectively active sites in the catalytic reactions, especially electrocatalysis[17]. Recently, MOFs were utilized as novel templates for the preparation of nanoporous carbons and metal oxides by direct carbonization of MOFs in inert atmospheres[18]. The MOFs-derived materials showed great potential in hydrogen storage[19], electrochemical capacitors[20] and lithium ion batteries[21]. Jiang and his coworkers synthesized a ZIF-8-derived nanoporous carbon material with an unexpectedly high surface area, considerable hydrogen storage capacity and good electrochemical properties as an electrode material for electric double layer capacitors[22]. Zhang et al reported a scalable synthesis of anisotropic hollow Fe_2O_3

[a] State Key Laboratory of Electroanalytical Chemistry, Changchun Institute of Applied Chemistry, Chinese Academy of Sciences, Changchun, Jilin, 130022 (China).
[b] University of Chinese Academy of Sciences, Beijing, 100049 (China).
† Corresponding author: Prof. Shaojun Dong, Email: E-mail: dongsj@ciac.ac.cn
Electronic Supplementary Information (ESI) available: [Additional information about TEM images of different catalysts, XRD comparision of NH_2-MIL-53(Fe) and other cobalt doped NH_2-MIL-53(Fe) and BET measurements of MOF(Fe_1-Co_3) and MOF(Fe_1-Co_3)$_{550N}$]. See DOI: 10.1039/x0xx00000x

microboxes by annealing prussian blue microcubes[23]. The as-synthesized Fe_2O_3 manifested high specific capacity (~950 mA·h·g^{-1} at 200mA·g^{-1}) and excellent cycling performance when used as anode material for lithium ion batteries. However, only a few works focused on electrochemically catalysis of OER by MOF-derived materials. Most of the reported MOF-derived OER catalysts are focused on direct carbonization of single transition metal-based MOFs[24], which exhibit limited catalytic activity towards OER.

In this work, Co-doped NH_2-MIL-53(Fe) has been directly carbonized in N_2 atmosphere and its electrochemical catalytic property toward OER in alkaline electrolyte has been investigated. The regular arrangement of metal ions and organic motifs in MOF structures leads to a uniform distribution of metal oxide nanoparticles, in situ formation of carbon species and pyridine N. The results showed that the OER efficiency was strongly dependent on the molar ratio of Fe and Co and the carbonization temperature. The Co-doped NH_2-MIL-53(Fe) annealed at 550 °C in an inert atmosphere with a molar ratio of Fe: Co = 1:3 (denoted as MOF$(Fe_1\text{-}Co_3)_{550N}$) showed the best electrocatalytic activity toward OER with an overpotential as low as 0.39 V at 10 mA·cm^{-2} and a Tafel slope of 72.9 mV·dec^{-1}, even comparable with the RuO_2 catalyst in alkaline electrolyte.

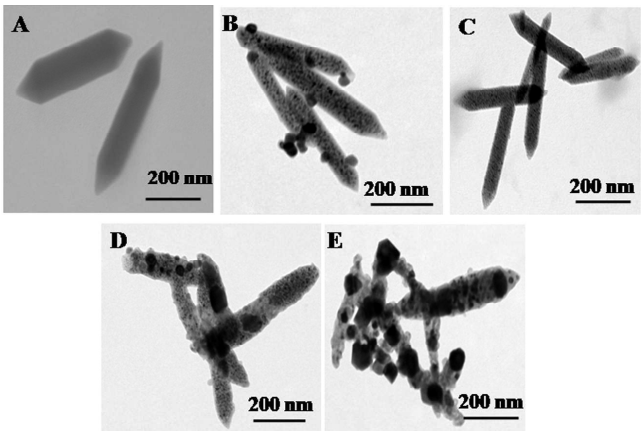

Figure 1. TEM images of MOF$(Fe_1\text{-}Co_3)$ calcinated at different temperatures. (A) MOF$(Fe_1\text{-}Co_3)$, (B) MOF$(Fe_1\text{-}Co_3)_{500N}$, (C) MOF$(Fe_1\text{-}Co_3)_{550N}$, (D) MOF$(Fe_1\text{-}Co_3)_{600N}$, and (E) MOF$(Fe_1\text{-}Co_3)_{700N}$.

Results and discussion

Characterization of Materials.

The as-prepared Co-doped NH_2-MIL-53(Fe) based materials were characterized by transmission electron microscopy (TEM). Figure S1 (Supporting Information) shows that the metal or metal oxide nanoparticles (M or MO_x) NPs in situ formed uniformly with size < 20 nm (especially, the diameter of M or MO_x NPs formed from MOF$(Fe_1\text{-}Co_3)_{550N}$ is *ca.*5 nm) and the skeleton of the Co-doped NH_2-MIL-53(Fe) is maintained (Figure S1).

To achieve the high electrocatalytic activity of Co-doped NH_2-MIL-53(Fe) toward oxygen evolution, the influences of molar ratios of Fe and Co and calcination temperature were investigated. Figure S2 B, C and D show that the sample size became longer and thinner obviously with increasing content of Co in the Co-doped NH_2-MIL-53(Fe). The calcination temperature is also an important factor which could influence the size of M or MO_x NPs. As shown in Figure 1, the morphologies of obtained-calcinates (MOF$(Fe_1\text{-}Co_3)$) under different temperatures (Figure 1B, C, D and E) were as same as the one before calcinations (Figure 1A). The results indicates that the M or MO_x NPs are uniformly formed at 550 ℃ (Figure 1C, the diameter of M or MO_x NPs is *ca.*5 nm), and when temperature is below or above 550 ℃, bulk M or MO_x NPs are formed on the surface of calcinates (Figure 1B, D and E). The framework structure of MOF$(Fe_1\text{-}Co_3)$ was destroyed when calcination at 600 °C and 700 °C (Figure 1D and E).Because of the low electrocatalytic efficiency of MOF$(Fe_1\text{-}Co_1)_{550N}$, MOF$(Fe_3\text{-}Co_1)_{550N}$, MOF$(Fe_1\text{-}Co_3)_{500N}$, MOF$(Fe_1\text{-}Co_3)_{600N}$ and MOF$(Fe_1\text{-}Co_3)_{700N}$ for OER (discussed detailed later), the following characterization just show the relative results of MOF$(Fe_1\text{-}Co_3)_{550N}$.

The chemical composition of MOF$(Fe_1\text{-}Co_3)_{550N}$ was confirmed by X-ray powder diffraction (XRD) and X-ray photoelectron spectroscopy (XPS). The atomic ratio of Co/Fe is determined to be 1.45 : 1 according to the ICP-OES result. Figure S3 showed that all the diffraction peaks of the as-prepared MOF$(Fe_x\text{-}Co_y)$ composites are consistent with the prepared NH_2-MIL-53(Fe), which indicated that the introduction of cobalt didn't influence the initial framework structure of NH_2-MIL-53(Fe). As shown in Figure 2A, the XRD pattern shows obvious Co_3O_4 peaks, indicating the formation of Co_3O_4 in MOF$(Fe_1\text{-}Co_3)_{550N}$.The peaks of Fe_2O_3 are relatively low because of the low content of Fe in MOF$(Fe_1\text{-}Co_3)_{550N}$ which is in coincidence with the result of XPS. As shown in the XPS full spectrum of MOF$(Fe_1\text{-}Co_3)_{550N}$ (Figure 2B), both MOF$(Fe_1\text{-}Co_3)$ and MOF$(Fe_1\text{-}Co_3)_{550N}$ showed the existence of C 1s, N 1s, O1s, Fe 2p and Co 2p. Figure 2C, 2D and 2E showed the deconvoluted spectra of Co 2p, Fe 2p and N 1s in the MOF$(Fe_1\text{-}Co_3)_{550N}$ sample. The deconvolution of Co 2p in Figure 2C showed the peak positions of Co $2p_{3/2}$ (780eV) and Co $2p_{1/2}$ (795 eV) are in good accordance with the presence of Co_3O_4[25]. The peaks at 711.3 and 724.9 eV are Fe $2p_{3/2}$ and Fe $2p_{1/2}$ (Figure 2D), respectively, which indicates the presence of Fe(III), and the satellite peak at the binding energy of 718.8 eV also corresponds to Fe(III)[26]. The deconvoluted N 1s spectrum is displayed in Figure 2E. The result shows that three kinds of N (pyridine N, pyrrole N and graphite N) existed in MOF$(Fe_1\text{-}Co_3)_{550N}$. It has been reported that the pyridinic and quaternary N atoms were active sites for the OER[27]. Hence, the enhancement of the OER activity attribute to the presence of the pyridine N.

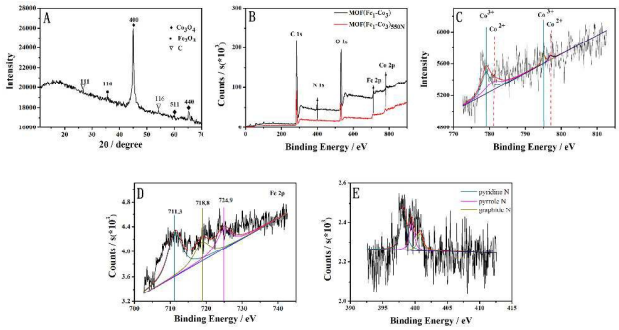

Figure 2 (A) XRD pattern of MOF(Fe_1-Co_3)$_{550N}$, (B) XPS full spectrum of MOF(Fe_1-Co_3) and MOF(Fe_1-Co_3)$_{550N}$, (C) deconvoluted Co 2p and (D) Fe 2p and (E)N 1s XPS spectra of MOF(Fe_1-Co_3)$_{550N}$.

The surface areas of as-prepared MOF(Fe_1-Co_3) and MOF(Fe_1-Co_3)$_{550N}$ were measured by Brunauer-Emmett-Teller (BET) method. Figure S4 illustrates the BET surface area of MOF(Fe_1-Co_3)$_{550N}$ (235.37 $m^2 \cdot g^{-1}$) is 4.35 times higher than that of MOF(Fe_1-Co_3) (54.03 $m^2 \cdot g^{-1}$). The curve of MOF(Fe_1-Co_3)$_{550N}$ sample shows the Type I isotherm with no obvious hysteresis, indicating the microporosity according to IUPAC classification. Such high surface area of MOF(Fe_1-Co_3)$_{550N}$ can provide more active sites to improve the OER efficiency. As shown in Figure S4, MOF(Fe_1-Co_3)$_{550N}$ shows mesopores centered at 12.25 nm and micropores centered at 3.5 nm, further implying the microporous structure in MOF(Fe_1-Co_3)$_{550N}$. What's more, the pores on the surface of MOF(Fe_1-Co_3)$_{550N}$ which connect with the cavity enable the catalyst contacting with the reactant at both the outer and inner surfaces and helping accelerate the diffusion of generated O_2.

Oxygen Evolution Activity.

Linear sweep voltammetry (LSV) was used to evaluate the electrochemical performance of the as-synthesized porous MOF(Fe_1-Co_3)$_{550N}$ for OER. It is very important to compare the overpotential for achieving the current density of 10 mA cm^{-2}, which is about 10% efficiency of solar-to chemical conversion. As shown in Figure 3A and B, in O_2-saturated 0.1 M KOH, the as-synthesized MOF(Fe_1-Co_3)$_{550N}$ presents higher OER current and lower applied potential at the OER current density of 10 mA·cm^{-2} (1.62 V) than other MOF(Fe_x-Co_y) composites. It is worth to note that the LSV curves of MOF(Fe_1-Co_3)$_{550N}$ and MOF(Fe_1-Co_1)$_{550N}$ were almost overlapped to each other (Figure 3A). The reasons are as follow. Firstly, the same content of N element was introduced during the experiment procedure. Secondly, the slight differences of the quantity of Co atoms dropped on the electrode (according to ICP-OES results, 6.38 • 10^{-8} M and 5.44 • 10^{-8} M, respectively) and the BET surface areas (235.37 $m^2 \cdot g^{-1}$ and 228.79 $m^2 \cdot g^{-1}$, respectively) between MOF(Fe_1-Co_3)$_{550N}$ and MOF(Fe_1-Co_1)$_{550N}$. Accordingly, the tiny differences of the content of active sites made the LSV curves of MOF(Fe_1-Co_3)$_{550N}$ and MOF(Fe_1-Co_1)$_{550N}$ nearly the same. The overpotential at MOF(Fe_1-Co_3)$_{550N}$ modified electrode is 0.39 V with a 10 mA·cm^{-2} current density, which is much close to that of the state-of-the art RuO_2 (0.38 V). The OER kinetics of the above catalysts are studied by Tafel plots (log j-E), as shown in Figure 3C. The Tafel slope for the MOF(Fe_1-Co_3)$_{550N}$ catalyst is about 72.9 mV·dec^{-1} which is better than other as-prepared composites and comparable to the RuO_2 catalyst (77.4 mV • dec^{-1}) (Figure 3C). The durability of the catalysts is significant in practical applications. The stability test was conducted with continuous cyclic potential scans in 0.1M KOH at a sweep rate of 100 mV s^{-1}. Compared to the overpotential increase of 23 mV for RuO_2 at the current density of 10 mA·cm^{-2}, 2 mV variation was observed at the MOF(Fe_1-Co_3)$_{550N}$ modified electrode after 1000 cycles (Figure 3D). The turnover frequency (TOC) was calculated to be 0.0033 s^{-1} (with an overpotential of 400 mV) and 0.0050 s^{-1} (with an overpotential of 450 mV).

The results suggest that the MOF(Fe_1-Co_3)$_{550N}$ exhibits excellent electrochemical OER catalytic ability which is comparable to the as-synthesized RuO_2.

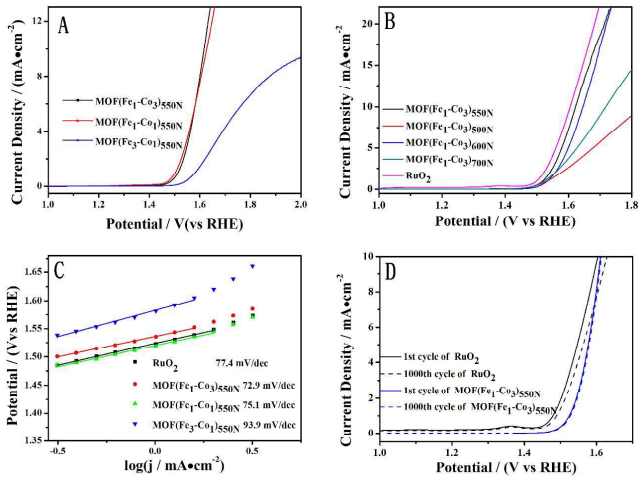

Figure 3 LSVs for different catalysts (A) (MOF(Fe_1-Co_3)$_{550N}$ (black line), MOF(Fe_1-Co_1)$_{550N}$ (red line), MOF(Fe_3-Co_1)$_{550N}$ (green line))and (B) (MOF(Fe_1-Co_3)$_{550N}$ (black line), MOF(Fe_1-Co_3)$_{500N}$ (red line), MOF(Fe_1-Co_3)$_{600N}$ (red line) MOF(Fe_1-Co_3)$_{700N}$ (green line) and RuO_2 (pink line)). (C) Tafel plot for different catalyst, and (D) OER polarization curves of MOF(Fe_1-Co_3)$_{550N}$ and RuO_2 before and after cyclic potential scans (1.0 – 2.0 V versus RHE) for 1000 cycles. All the experiments are performed on a RDE (1600 rpm) in an O_2-saturated 0.1 M KOH solution (scan rate: 5 mV·s^{-1} for LSVs and 1 mV·s^{-1} for Tafel plot).The calculation of the OER current density was based on the geometric surface area.

Experimental

Materials. $Fe(NO_3)_3 \cdot 6H_2O$, $Co(NO_3)_2 \cdot 6H_2O$, sodium hydroxide (NaOH) and dimethylformamide (DMF) were purchased from Beijing Chemical Corp. 2-aminoterephthalate (H_2ATA) were purchased from Alfa Aesar. Nafion (5.0 wt %) and $RuCl_3 \cdot 3H_2O$ were purchased from Sigma–Aldrich. All chemicals used were of analytical grade and used without further purification. Milli-Q ultrapure water (Millipore, ⩾18.2 M Ω· cm) was used throughout the experiments.

Characterization. Transmission electron microscopy (TEM) was performed on a HITACHI H-600 Analytical TEM with an accelerating voltage of 100 kV. X-ray powder diffraction (XRD) patterns were recorded on a D8 ADVANCE (BRUKER, Germany) diffractometer using Cu −Kα radiation with a Ni filter (λ =0.154059 nm at 30 kV and 15 mA). X-ray photoelectron spectroscopy (XPS) measurement was performed on an ESCALAB-MKI I spectrometer (VG Co., United Kingdom) with Al Kα X-ray radiation as the X-ray source for excitation. The exact composition of Co/Fe in the as-prepared MOF$(Fe_1\text{-}Co_3)_{550N}$ was determined by an inductively coupled plasma optical emission spectrometer (ICP-OES, X Series 2, Thermo Scientific USA). Brunauer-Emmett-Teller (BET) surface areas and Nitrogen sorption isotherms were measured with an ASAP 2020 Physisorption Analyzer (Micrometrics Instrument Corporation).

All the electrocatalytic measurements were performed with a CHI 832c electrochemical workstation (Chenhua Instruments Corp, Shanghai, China) at room temperature. Rotating disk electrode (RDE) technique was employed on a Model RRDE-3A Apparatus (BAS, Japan) with a CHI832c electrochemical workstation. A conventional three-electrode cell was used, including a KCl saturated Ag/AgCl electrode as reference electrode, a platinum wire as counter electrode, and a rotating disk electrode of glassy carbon (RDE) with a diameter of 3.0 mm as working electrode, respectively.

Synthesis of Co-doped NH_2-MIL-53(Fe). Co-doped NH_2-MIL-53(Fe) was prepared as described previously with some modification[25]. In a typical procedure, 1 mmol of $Fe(NO_3)_3{\cdot}6H_2O$, 3mmol of $Co(NO_3)_2{\cdot}6H_2O$ and 1 mmol of H_2ATA were added slowly into 10 mL of DMF solution. The mixture was stirred for 10 min at room temperature followed by transferred into a Teflon-lined stainless steel autoclave (with volume of 50 mL) and heated at 150 °C for 6 h. After cooled naturally to room temperature, the mixture was centrifugated at 6000 rpm for 5 minutes and the precipitate was purified with methanol and water successively and dried in vacuum at 60 °C for 24 h, denoted as MOF$(Fe_1\text{-}Co_3)$. Adjusting the amount of $Fe(NO_3)_3{\cdot}6H_2O$ and $Co(NO_3)_2{\cdot}6H_2O$, we synthesized different molar ratios of Fe and Co MOF, denoted as MOF$(Fe_3\text{-}Co_1)$ and MOF$(Fe_1\text{-}Co_1)$.

Carbonization of Co-doped NH_2-MIL-53(Fe). Under N_2 flow, the as-obtained MOF$(Fe_1\text{-}Co_3)$ was carbonized at 550 ℃ for 2h with the heating rate of 10 °C /min. The obtained black powder was denoted as MOF$(Fe_1\text{-}Co_3)_{550N}$ composite. For comparison, MOF$(Fe_1\text{-}Co_3)$ was also carbonized at 500, 600 and 700 °C under the same condition, denoted as MOF$(Fe_1\text{-}Co_3)_{500N}$, MOF$(Fe_1\text{-}Co_3)_{600N}$ and MOF$(Fe_1\text{-}Co_3)_{700N}$, respectively.

MOF$(Fe_3\text{-}Co_1)$ and MOF$(Fe_1\text{-}Co_1)$ were also treated at 550 ℃ under the same condition with MOF$(Fe_1\text{-}Co_3)$, denoted as MOF$(Fe_3\text{-}Co_1)_{550N}$, MOF$(Fe_1\text{-}Co_1)_{550N}$, respectively. The results showed MOF$(Fe_x\text{-}Co_y)_{550N}$ composites are uniform, monodispersed spindle-like structure (Figure S1) which preserved the original morphology of NH_2-MIL-53(Fe) (Figure S2 A, Supporting Information).

Synthesis of RuO_2. The RuO_2 was prepared as described before[26]. An aqueous solution containing 0.01 mol of $RuCl_3{\cdot}3H_2O$ was heated （100 °C) with magnetical stirring for 10 min, then 1 mL of NaOH (1 M) was added to the solution in order to obtain the precursor Ru-hydroxide. The obtained mixture kept heating at 100 °C for 45 min under stirring, then the precipitate was washed several times and calcined at 350 °C for 1 h to obtain the RuO_2. The as-prepared RuO_2 was chacterized by XPS and TEM (Figure S5).

Electrochemical Measurements. All the measurements were carried out at room temperature. The electrochemical measurement of OER was measured by a Model RRDE-3A Apparatus (BAS, Japan) with a CHI832c electrochemical workstation. A RDE was used as working electrode for the test of OER activity. A KCl saturated Ag/AgCl electrode was used as the reference electrode and was calibrated with respect to a RHE ($E_{RHE} = E_{Ag/AgCl} + 0.059\ pH + 0.197$) and Pt wire were used as the working and counter electrodes, respectively.

Before modification, RDE was polished with 1, 0.3 and 0.05 μm alumina slurry, respectively. Then, it was washed successively with alcohol/water (1:1) mixture in an ultrasonic bath and dried in air. For a typical procedure, 1.0 mg of the MOF$(Fe_1\text{-}Co_1)_{500N}$ or RuO_2 catalyst was dispersed in a mixture (0.5 mL) of water, isopropyl alcohol, and Nafion (5.0 wt %) with a ratio of 20:1:0.75 (v/v/v) under sonication. In the RDE system, a certain amount of MOF$(Fe_1\text{-}Co_3)_{550N}$ solution was casted onto the pretreated RDE surface (142 $\mu g/cm^2$). For comparison, the RuO_2 modified RDE (RuO_2/RDE) was prepared under the same procedure with an amount of catalyst (71 $\mu g\ /cm^2$).

In RDE measurements, linear sweep voltammetry (LSV) were conducted in an oxygen-saturated KOH solution (pH 13) at room temprature using a scan rate of $5mV{\cdot}s^{-1}$ and a rotation speed of 1600 rpm (BAS, Japan). All LSV polarization curves were corrected with 95% iR-compensation.

Furthermore, the turnover frequency (TOF) was calculated based on all the cobalt ions dropped on the electrode rather than the cobalt ions on the surface of the electrode. TOF was calculated according to equation: TOF = j*A/(4*F*m), where j is the current density obtained at overpotential of 400mV and 450 mV, A is the surface area of the electrode, F is the Faraday efficiency (96,000 $C{\cdot}mol^{-1}$) and m is the number of moles of the cobalt ions dropped onto the electrode. The mole number of cobalt ions was quantified through ICP-OES result.

Conclusions

In summary, by one-step carbonization of cobalt doped NH_2-MIL-53(Fe), we successfully synthesized the porous MOF-derived complexes which show outstanding electrochemical activity toward oxygen evolution catalysis. The MOF$(Fe_1\text{-}Co_3)_{550N}$ shows the highest OER electrocatalytic efficiency among the as-obtained materials. The results of characterization showed that, the MOF$(Fe_1\text{-}Co_3)_{550N}$ presents a spidle-like 3D structure with a large surface area and mesopores in the material, and the formation of pyridine N and Co_3O_4 are the key factors which could boost the performance of OER activity. The overpotential of 0.39 V at the current density of 10 $mA{\cdot}cm^{-2}$ with a large anodic current, and the Tafel slope of 72.9 $mV{\cdot}dec^{-1}$ in alkaline solution are

obtained through LSV. The favorable OER performance is comparable to the as-synthesized RuO_2. The MOF$(Fe_1\text{-}Co_3)_{550N}$ catalyst also possesses better stability than as-prepared RuO_2 under serious cyclic potential scans. Such novel designed MOF-based materials in this work provide a facile and universal way to enrich families of OER electrocatalysts and can be extended by doping other transition metals, such as nickel, manganese and titanium, and other heteroatoms, such as boron, phosphorus and sulphur, in MOFs.

Acknowledgements

This work was supported by the National Natural Science Foundation of China (No. 21375123), the 973 Project (No. 2011CB911002) and the Ministry of Science and Technology of China (No. 2013YQ170585).

Notes and references

[1] R. G. Gonzalez-Huerta, G. Ramos-Sanchez, P. B. Balbuena, *J. Power Sources* **2014**, *268*, 69-76.

[2] D. Galizzioli, F. Tantardini' and S. Trasatti, *J Appl. Electrochem*. **1974**, *57*-67.

[3] Y. Zhu, W. Zhou, Y. Chen, J. Yu, M. Liu, Z. Shao, *Adv Mater* **2015**, DOI: 10.1002/adma.201503532.

[4] Z. Y. Lu, H. T. Wang, D. S. Kong, K. Yan, P. C. Hsu, G. Y. Zheng, H. B. Yao, Z. Liang, X. M. Sun, Y. Cui, *Nat. Commun.* **2014**, *5*.

[5] R. Subbaraman, D. Tripkovic, K. C. Chang, D. Strmcnik, A. P. Paulikas, P. Hirunsit, M. Chan, J. Greeley, V. Stamenkovic, N. M. Markovic, *Nat. Mater.* **2012**, *11*, 550-557.

[6] a)H. S. Ahn, A. J. Bard, *J. Am. Chem. Soc.* **2015**, *137*, 612-615; b)X. B. Han, Z. M. Zhang, T. Zhang, Y. G. Li, W. B. Lin, W. S. You, Z. M. Su, E. B. Wang, *J. Am. Chem. Soc.* **2014**, *136*, 5359-5366.

[7] a)C. S. Lim, C. K. Chua, Z. Sofer, O. Jankovsky, M. Pumera, *Chem. Mate.* **2014**, *26*, 4130-4136; b)M. X. Shen, C. P. Ruan, Y. Chen, C. H. Jiang, K. L. Ai, L. H. Lu, *ACS Appl. Mater. Interfaces.* **2015**, *7*, 1207-1218.

[8] a)Y. L. Zhu, W. Zhou, Z. G. Chen, Y. B. Chen, C. Su, M. O. Tade, Z. P. Shao, *Angew. Chem. Int. Edit.* **2015**, *54*, 3897-3901. b) W. Zhou, M. Zhao, F. Liang, S. C. Smith, Z. Zhu, Mater. Horiz.,2015, 2,495—501. c) X. Xu, C. Su, W. Zhou, Y. Zhu, Y. Chen, Z. Shao, Adv. Sci. 2015, 1500187.

[9] a)Q. S. Yin, J. M. Tan, C. Besson, Y. V. Geletii, D. G. Musaev, A. E. Kuznetsov, Z. Luo, K. I. Hardcastle, C. L. Hill, *Science* **2010**, *328*, 342-345; b)V. Artero, M. Chavarot-Kerlidou, M. Fontecave, *Angew. Chem. Int. Edit.* **2011**, *50*, 7238-7266.

[10] a)F. Jiao, H. Frei, *Energy Environ. Sci.* **2010**, *3*, 1018-1027; b)F. Jiao, H. Frei, *Angew. Chem. Int. Edit.* **2009**, *48*, 1841-1844; c)N. Jiang, B. You, M. L. Sheng, Y. J. Sun, *Angew. Chem. Int. Edit.* **2015**, *54*, 6251-6254.

[11] I. C. Man, H. Y. Su, F. Calle-Vallejo, H. A. Hansen, J. I. Martinez, N. G. Inoglu, J. Kitchin, T. F. Jaramillo, J. K. Norskov, J. Rossmeisl, *ChemCatChem* **2011**, *3*, 1159-1165.

[12] J. Suntivich, K. J. May, H. A. Gasteiger, J. B. Good enough, Y. Shao-Horn, *Science* **2011**, 334, 1383-1385.

[13] a)Z. J. Zhang, H. T. H. Nguyen, S. A. Miller, S. M. Cohen, *Angew. Chem. Int. Edit.* **2015**, *54*, 6152-6157; b)A. Karmakar, A. V. Desai, B. Manna, B. Joarder, S. K. Ghosh, *Chem. Eur. J.* **2015**, *21*, 7071-7076; c)F. Ragon, H. Chevreau, T. Devic, C. Serre, P. Horcajada, *Chem. Eur. J* **2015**, *21*, 7135-7143.

[14] a)Y. H. Ren, M. Y. Wang, X. Y. Chen, B. Yue, H. Y. He, *Materials* **2015**, *8*, 1545-1567; b)F. M. Zhang, Y. Jin, J. Shi, Y. J. Zhong, W. D. Zhu, M. S. El-Shall, *Chem. Eng. J.* **2015**, *269*, 236-244.

[15] a)J. Duan, W. Jin, R. Krishna, *Inorg. Chem.* **2015**, *54*, 4279-4284; b)A. Buragohain, S. Biswas, *Eur. J. Inorg. Chem.* **2015**, 2463-2468.

[16] a)V. B. Pokharkar, M. R. Jolly, D. D. Kumbhar, *Eur. J. Pharm. Sci.* **2015**, *71*, 99-111; b)Q. L. Li, J. P. Wang, W. C. Liu, X. Y. Zhuang, J. Q. Liu, G. L. Fan, B. H. Li, W. N. Lin, J. H. Man, *Inorg. Chem. Commun.* **2015**, *55*, 8-10.

[17] a)D. D. Zhu, L. J. Li, J. J. Cai, M. Jiang, J. B. Qi, X. B. Zhao, *Carbon* **2014**, *79*, 544-553; b)W. Zhang, Z. Y. Wu, H. L. Jiang, S. H. Yu, *J. Am. Chem. Soc.* **2014**, *136*, 14385-14388; c)M. Jahan, Z. L. Liu, K. P. Loh, *Adv. Funct. Mater.* **2013**, *23*, 5363-5372; d)A. Morozan, F. Jaouen, *Energy Environ. Sci.* **2012**, *5*, 9269-9290.

[18] a)M. B. Zakaria, M. Hu, R. R. Salunkhe, M. Pramanik, K. Takai, V. Malgras, S. Y. Choi, S. X. Dou, J. H. Kim, M. Imura, S. Ishihara, Y. Yamauchi, *Chem. Eur. J* **2015**, *21*, 3605-3612; b)W. Xia, R. Q. Zou, L. An, D. G. Xia, S. J. Guo, *Energy Environ. Sci.* **2015**, *8*, 568-576; c)Y. H. Song, X. Li, C. T. Wei, J. Y. Fu, F. G. Xu, H. L. Tan, J. Tang, L. Wang, *Sci. Rep.* **2015**, *5*.

[19] a)J. A. Villajos, G. Orcajo, C. Martos, J. A. Botas, J. Villacanas, G. Calleja, *Int. J. Hydrogen. Energ.* **2015**, *40*, 5346-5352; b)M. G. Campbell, D. Sheberla, S. F. Liu, T. M. Swager, M.

Dinca, *Angew. Chem. Int. Edit.* **2015**, *54*, 4349-4352; cJ. N. Hao, B. Yan, *Chem. Commun.* **2015**, *51*, 7737-7740.

[20] a)X.-Y. Yu, L. Yu, H. B. Wu, X. W. D. Lou, *Angew. Chem. Int. Edit.* **2015**, *54*, 5331-5335; b)K. M. Choi, H. M. Jeong, J. H. Park, Y. B. Zhang, J. K. Kang, O. M. Yaghi, *Acs Nano* **2014**, *8*, 7451-7457.

[21] a)G. H. Zhang, S. C. Hou, H. Zhang, W. Zeng, F. L. Yan, C. C. Li, H. G. Duan, *Adv. Mater.* **2015**, *27*, 2400-2405; b)G. Huang, F. F. Zhang, X. C. Du, Y. L. Qin, D. M. Yin, L. M. Wang, *Acs Nano* **2015**, *9*, 1592-1599.

[22] H. L. Jiang, B. Liu, Y. Q. Lan, K. Kuratani, T. Akita, H. Shioyama, F. Zong, Q. Xu, *J. Am. Chem. Soc.* **2011**, *133*, 11854-11857.

[23] L. Zhang, H. B. Wu, S. Madhavi, H. H. Hng, X. W. Lou, *J. Am. Chem. Soc.* **2012**, *134*, 17388-17391.

[24] a)J. S. Li, S. L. Li, Y. J. Tang, M. Han, Z. H. Dai, J. C. Bao, Y. Q. Lan, *Chem. Commun.* **2015**, *51*, 2710-2713; b)T. Y. Ma, S. Dai, M. Jaroniec, S. Z. Qiao, *J. Am. Chem. Soc.* **2014**, *136*, 13925-13931.

[25] W. Song, A. S. Poyraz, Y. Meng, Z. Ren, S.-Y. Chen, S. L. Suib, *Chem. Mater.* **2014**, *26*, 4629-4639.

[26] N. Cheng, Q. Liu, J. Tian, Y. Xue, A. M. Asiri, H. Jiang, Y. He and X. Sun, *Chem. Commun.* **2015**, 51, 1616-1619.

[27] Y. Zhao, R. Nakamura, K. Kamiya, S. Nakanishi, K. Hashimoto, *Nat. Commun.* **2013**, *4*, 2390.